

Are Waters around RNA More than Just a Solvent? – An Insight from Molecular Dynamics Simulations

Petra Kührová,[†] Michal Otyepka,^{†,‡} Jiří Šponer,^{‡,§} and Pavel Banáš*,^{†,‡}

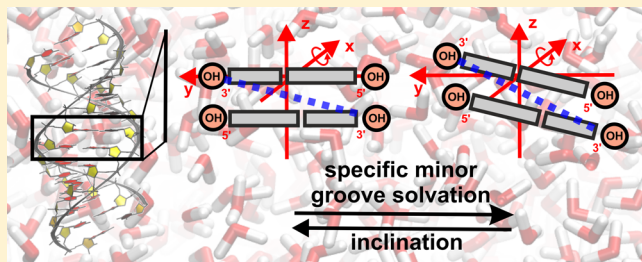
[†]Regional Centre of Advanced Technologies and Materials, Department of Physical Chemistry, Faculty of Science, Palacky University, tr. 17. Listopadu 12, 771 46, Olomouc, Czech Republic

[‡]Institute of Biophysics, Academy of Sciences of the Czech Republic, Kralovopolska 135, 612 65 Brno, Czech Republic

[§]CEITEC – Central European Institute of Technology, Campus Bohunice, Kamenice 5, 625 00 Brno, Czech Republic

Supporting Information

ABSTRACT: Hydrating water molecules are believed to be an inherent part of the RNA structure and have a considerable impact on RNA conformation. However, the magnitude and mechanism of the interplay between water molecules and the RNA structure are still poorly understood. In principle, such hydration effects can be studied by molecular dynamics (MD) simulations. In our recent MD studies, we observed that the choice of water model has a visible impact on the predicted structure and structural dynamics of RNA and, in particular, has a larger effect than type, parametrization, and concentration of the ions. Furthermore, the water model effect is sequence dependent and modulates the sequence dependence of A-RNA helical parameters. Clearly, the sensitivity of A-RNA structural dynamics to the water model parametrization is a rather spurious effect that complicates MD studies of RNA molecules. These results nevertheless suggest that the sequence dependence of the A-RNA structure, usually attributed to base stacking, might be driven by the structural dynamics of specific hydration. Here, we present a systematic MD study that aimed to (i) clarify the atomistic mechanism of the water model sensitivity and (ii) discover whether and to what extent specific hydration modulates the A-RNA structural variability. We carried out an extended set of MD simulations of canonical A-RNA duplexes with TIP3P, TIP4P/2005, TIP5P, and SPC/E explicit water models and found that different water models provided a different extent of water bridging between 2'-OH groups across the minor groove, which in turn influences their distance and consequently also inclination, roll, and slide parameters. Minor groove hydration is also responsible for the sequence dependence of these helical parameters. Our simulations suggest that TIP5P is not optimal for RNA simulations.



INTRODUCTION

An accurate description of the structure of the hydration shells surrounding biomolecules is important for understanding most molecular processes, ranging from folding and assembly of proteins and nucleic acids to molecular recognition and binding of small molecules. A solvation layer of water molecules plays a crucial role in the function of biological systems, both indirectly, by stabilizing native conformations of biomolecules, and directly, by actively participating in biological processes.¹

The polyanionic nature of nucleic acids induces stronger interactions with solvent molecules (both ions and waters) than for proteins. The solvent distribution in the minor and major grooves of nucleic acid duplexes is structured in specific sequence dependent patterns. Water molecules located in the grooves have relatively long residence times, ranging from tens of picoseconds up to nanoseconds.^{2–8} The combination of well-ordered water molecules in the first hydration shell and their long residence times means that the hydrating waters can be considered an integral part of nucleic acid structures.⁹ The distribution of water molecules helps to stabilize A-RNA duplexes and plays an important role in RNA/RNA and

protein/RNA recognition processes.¹⁰ The interactions of water with proteins and nucleic acids have been extensively studied both experimentally^{11–16} and computationally.^{17–29} The hydration patterns around RNA Watson–Crick and non-Watson–Crick base pairs and unpaired RNA bases in X-ray structures have been analyzed and described in several studies.^{11–14,17,30} Crystallography has unambiguously established that some water molecules occupy spatially well-defined hydration sites in the vicinity of nucleic acid atoms.^{9,10,30} Unfortunately, even for high resolution structures, not all of these hydration sites are visible.

Molecular dynamics (MD) simulations, when used insightfully with enough attention paid to force field limitations, can provide unique information that complements experimental data.^{31,32} However, the RNA force field and simulation protocols still remain somewhat underdeveloped compared to protein simulations.^{33–35} Besides the RNA force field, solvent and ionic conditions may affect the outcome of the simulations.

Received: July 26, 2013

Published: November 22, 2013



There is increasing evidence that the effect of ions (i.e., their type, parameters, and concentration) on RNA structural dynamics in MD simulations is considerably smaller than previously assumed.^{36,37} On the other hand, the choice of water model has been shown to have a considerable effect on RNA simulations.^{21,36,38}

The selection of a realistic water model is crucial for the success of simulations in an environment of explicit water molecules and has been the subject of intensive research over many decades.^{39,40} It should be noted that current implicit solvent models cannot be used for productive MD simulations of RNA because they lead to rapid unfolding of folded RNA molecules, as shown, e.g., for the *glmS* riboswitch.⁴¹ During recent years, new explicit water models or reparameterizations of old ones have been published.^{42–49} Explicit water models should fulfill two general conditions: (i) generality of the model, i.e., the model should perform well in a large set of properties for a wide range of conditions, and (ii) simplicity of the model, which is necessary to keep computational costs low. Every explicit water model is parametrized and tested against its ability to reproduce as much as possible experimentally determined physicochemical properties of bulk water, such as structure, density, enthalpy of vaporization, self-diffusion rate, or dielectric constant. However, water potentials derived to represent bulk water properties may not accurately represent the properties of water molecules in the hydration shell of biomolecules. Thus, the optimal water model should accurately reproduce the properties of both bulk and hydration shell waters. Currently, the most popular water models used for contemporary MD simulations of biomolecules are Jorgensen's TIPnP^{44,50,51} and Berendsen's SPC/E⁵² explicit water models. For protein and nucleic acid simulations, three site models (TIP3P and SPC/E) are predominantly used due to their relatively low computational costs in comparison with four (e.g., TIP4P) and five (e.g., TIP5P) site models. Explicit water models have recently been tested and compared on various systems. These studies have shown that the choice of explicit water model affects the predicted structural dynamics of simulated biomolecules.^{28,34,36,53–57} Florova and co-workers⁵³ have shown that the explicit water model significantly influences the structural dynamics of unstructured parts of a protein, whereas the tightly folded region remains insensitive to the choice of water model. These findings have especial relevance for simulations of intrinsically disordered proteins that are inherently unstructured as the water model choice is likely to have a significant influence on the simulation behavior of these systems.⁵⁸

In this study, we performed a set of MD simulations of canonical A-RNA duplexes with different sequences using four explicit solvent models (TIP3P, TIP4P/2005, TIPSP, and SPC/E), two of which (TIP4P/2005 and TIPSP), to the best of our knowledge, were used for the first time in RNA simulations. We aimed to analyze two effects connected to the specific solvation of A-RNA duplexes: (i) identification of the mechanism, i.e., how the choice of specific explicit water model affects the A-RNA helical structure, and (ii) investigation of the sequence dependent variation of the helical structure of A-RNA duplexes observed in MD simulations.³⁶ Regarding the sequence dependence of the A-RNA structure, we concentrated on testing two different hypotheses suggested in our recent study,³⁶ namely that the effect is caused either by (i) the steric shape of nucleotides via intramolecular stacking (mainly interstrand steric clashes) or (ii) by specific hydration in the

minor groove. It should be noted that we focused on determining the role of specific hydration on the sequence dependence of helical parameters rather than comparing the performance of the studied water models in the description of such sequence dependence, as this comparison would be significantly limited by the lack of available experimental structural data.³⁸

METHODS

Simulation Protocol. Classical MD simulations of canonical A-RNA duplexes were carried out with several explicit water models using the AMBER⁵⁹ package with the all-atomic *ff99bsc0χOL3* force field.^{33,60} The *ff99bsc0χOL3* force field is based on the AMBER *ff99*⁶¹ force field corrected by Barcelona α/γ ⁶² and Olomouc χ_{OL3} ³³ reparameterizations (included as standard in the AMBER RNA force field since 2010). We employed the most popular explicit water models currently available: TIP3P,⁵⁰ TIP4P/2005,⁶³ TIPSP,⁴⁴ and SPC/E.⁵² Systems were immersed in a rectangular box with at least 10 Å between the solute and box wall. Na⁺ or K⁺ ions were used to neutralize the RNA structure (26 counterions). Excess salt simulations were performed by the addition of Cl⁻, appropriate cations (Na⁺ or K⁺), and Mg²⁺ ions (14 Cl⁻, 40 K⁺, and 4 Mg²⁺, respectively, corresponding to 150 mM KCl/NaCl and 20 mM MgCl₂). The ion parameters for each explicit water model were as follows: Na⁺ (TIPnP: $r = 1.369$ Å, $\epsilon = 0.0874$ kcal/mol; TIP4P/2005: $r = 1.226$ Å, $\epsilon = 0.1684$ kcal/mol; SPC/E: $r = 1.212$ Å, $\epsilon = 0.3526$ kcal/mol),⁶⁴ K⁺ (TIPnP: $r = 1.705$ Å, $\epsilon = 0.1937$ kcal/mol; TIP4P/2005: $r = 1.590$ Å, $\epsilon = 0.2795$ kcal/mol; SPC/E: $r = 1.593$ Å, $\epsilon = 0.4297$ kcal/mol),⁶⁴ Cl⁻ (TIPnP: $r = 2.513$ Å, $\epsilon = 0.0355$ kcal/mol; TIP4P/2005: $r = 2.760$ Å, $\epsilon = 0.0117$ kcal/mol; SPC/E: $r = 2.711$ Å, $\epsilon = 0.0127$ kcal/mol),⁶⁴ and Mg²⁺ ($r = 1.5545$ Å, $\epsilon = 0.00295$ kcal/mol).⁶⁵ The simulation length was 200 ns, which has been shown to give sufficient convergence for A-RNA duplexes.³⁶ In addition, two independent 200 ns runs were calculated for the simulations of short duplexes (see below). Details of all simulations used in this study, together with information about the explicit water models, are listed in the Supporting Information (Table S1). We used a standard simulation protocol, which has repeatedly been shown to perform well for various RNA systems.^{34,36,37,41,60,66,67} The simulation protocol is also described in the Supporting Information.

Studied Systems. The following A-RNA canonical Watson–Crick (i.e., containing CG and AU base pairs) duplexes were chosen as model systems for detailed analysis of the relationship between water model choice and helical parameters of RNA duplexes: short r(CGCG) duplex and duplexes with repetitive sequences also used in ref 36, i.e., r(CG)₅, r(CG)₇, r(AU)₇, r(GA)₇, r(GU)₇, r(A)₁₄, and r(G)₁₄. These canonical structures were built using the INSIGHT II program package (Biosym/MSI, San Diego, CA, October 1995) and thus represent an idealized A-form RNA duplex. In addition, we carried out simulations of a decamer sequence r(GCACCGUUGG) excised from a 19 base-pair A-RNA duplex deposited under PDB code 1QC0⁶⁸ with a resolution of 1.55 Å. All simulations presented in this paper are new, as we used a different box than in ref 36 to simplify the hydration analyses. Note that although the starting structures could potentially significantly influence the simulation behavior, the effects studied here, i.e., local variations of the A-form helical structure reflected in a rather gentle shift of helical parameters, are reportedly converged within tens or a few hundred of

nanoseconds.³⁶ In addition, all artificial sequences started from an idealized A-form duplex, and thus the observed effects (differences) can be confidently attributed to the system and/or force field.

Unphysical Hybrid r(A/D)₁₄-Tract. In order to identify the source of the sequence dependence of helical parameters of A-RNA duplexes, we performed simulations of the r(A/D)₁₄-tract. This is an unphysical hybrid A-RNA system mixing interactions and parameters of the r(D)₁₄-tract and r(A)₁₄-tract (D stands for diaminopurine, which is paired with uracil via the DU base pair, see ref 36). The van der Waals component of the intramolecular (i.e., intraduplex) RNA–RNA interactions of this hybrid system (involving, *inter alia*, stacking, and base pairing) corresponds to r(D)₁₄-tract interactions, whereas the RNA–solvent interactions and electrostatic part of the RNA–RNA intramolecular interactions correspond to the r(A)₁₄-tract. In other words, van der Waals stacking interactions sense the N2-exocyclic amino groups of diaminopurines, whereas solvent molecules sense unperturbed adenines at the same places (see Figure S1 and Supporting Information). Note that for technical reasons, we were not able to split the electrostatic interaction like the van der Waals component (i.e., into r(D)₁₄-tract-like RNA–RNA interactions and r(A)₁₄-tract-like RNA–solvent interactions). However, we assumed that this would not significantly affect r(D)₁₄-tract-like base stacking as the stacking interaction is dominantly driven by the van der Waals term. On the other hand, such a hybrid description of RNA–RNA interactions affects the base pairing of the DU pair; namely, the lack of electrostatics in the D(N2)…U(O2) hydrogen bond results in a repulsive interaction between the bulky N2-exocyclic amino group of D (described only by van der Waals spheres, not by charges) and the U(O2) carbonyl group. Therefore, we restrained the conformations of DU/AU base pairs of this hybrid system to mimic the isosteric conformations of DU and AU base pairs (see Figure S7 and Supporting Information for more details). This “alchemical” model system allowed the roles of the different contributions to be separated in the studied systems.

Analyses of Simulations. The global behavior of each system was analyzed using the *ptraj* module (AMBER tool). Helical parameters were monitored using the X3DNA program.⁶⁹ In addition, the X3DNA program was used to evaluate dihedral backbone angles and sugar pucker. The number of bridging water molecules forming an uninterrupted chain of hydrogen bound water molecules connecting two 2'-OH groups across the minor groove was calculated using in-house software, where we used the following criterion for a hydrogen bond: the distance of heavy atoms should be below 3.5 Å, and the hydrogen–hydrogen donor–hydrogen acceptor angle should be below 40°.

RESULTS AND DISCUSSION

Our recent studies have indicated that the choice of explicit solvent model in MD simulations has a significant effect on the predicted helical structure of canonical A-form RNA duplexes as well as on the structural dynamics of some noncanonical RNA systems.^{36–38} The effect of the water model was found to be visibly more important than the effects of ionic conditions (type and concentration of ions),^{36,37} albeit still much smaller than the effect of the solute force field parametrization.^{36,38} We have also shown that the helical structure of the A-RNA duplex is sequence dependent, with, e.g., inclination of the base pairs varying over the range 10° to 24°. Similarly, the sensitivity of

helical parameters of A-RNA to the choice of water model is sequence dependent. Both of these dependencies correlate with the hydrogen bonding pattern in the minor groove, i.e., the presence or absence of a purine N2-amino group.³⁶

Effect of Water Model Choice on Helical Structure of A-RNA Duplex. Influence of Water Model on Behavior of the 2'-Hydroxyl Group. While previous studies have suggested the sensitivity of simulations of nucleic acids to the water model, none have analyzed the origin (mechanism on atomistic level) of this effect.^{36–38} Our preceding A-RNA study comparing TIP3P and SPC/E waters demonstrated that the effect of the water model is sequence dependent, correlating with the minor groove rather than major groove hydrogen bonding pattern.³⁶ Furthermore, it was shown that simulations of a B-DNA duplex are less sensitive to the water model choice.⁷⁰ These observations indicate that phosphate groups exposed to the major groove of the A-RNA helix are less likely to be responsible for the sensitivity of A-RNA simulations to the water model choice. Instead, the 2'-hydroxyl groups exposed to the minor groove and directly interacting with water molecules solvating the minor groove might mediate the effect of explicit solvent models. In other words, different water models might induce different orientations of the 2'-OH groups, which in turn might locally affect helical parameters of A-form duplexes. Assuming puckering of the C3'-endo sugar, the 2'-OH group can populate three different orientations (Figure 1): (a) toward O4', where the orientation is stabilized

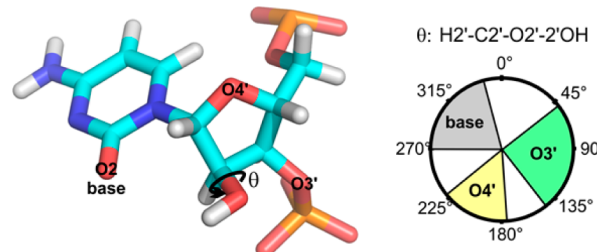


Figure 1. Orientation of the 2'-hydroxyl group. The structure depicted shows the torsion angle H2'-C2'-O2'-2'OH with three favored orientations: toward O3', O4', or the base domain. The conformation wheel represents the distribution of the torsion angle for the C3'-endo sugar conformation. The torsion angle θ populates three regions: O3' domain with torsion angle $\theta = 50\text{--}140^\circ$, O4' domain with torsion angle $\theta = 175\text{--}230^\circ$, and base domain with torsion angle $\theta = 270\text{--}345^\circ$.

by favorable intraribose electrostatic interactions with the O4' oxygen (O4' domain), (b) toward O3', where the 2'-OH forms a hydrogen bond with the O3' oxygen (O3' domain), and (c) toward the sugar edge of the base, where the 2'-OH group is hydrogen bonded to the water molecule bound to the purine N3 or pyrimidine O2 atoms, respectively (base domain).^{71,72} It is worth noting that the base domain is the biochemically most interesting orientation and is responsible for the heterogeneity of RNA structures because it offers the 2'-OH into a wide range of key “sugar edge” H-bond RNA–RNA interactions directing the conformation of folded RNAs.⁷³ Nevertheless, in canonical A-RNA, which is the focus of our study, the 2'-OH group does not have a relevant partner nucleotide for sugar-edge RNA–RNA interactions. In A-RNA, a hydrogen bond between the 2'-OH group and the above-mentioned structural water in the minor groove is present in all orientations of the hydroxyl group. However, whereas the 2'-hydroxyl group donates a

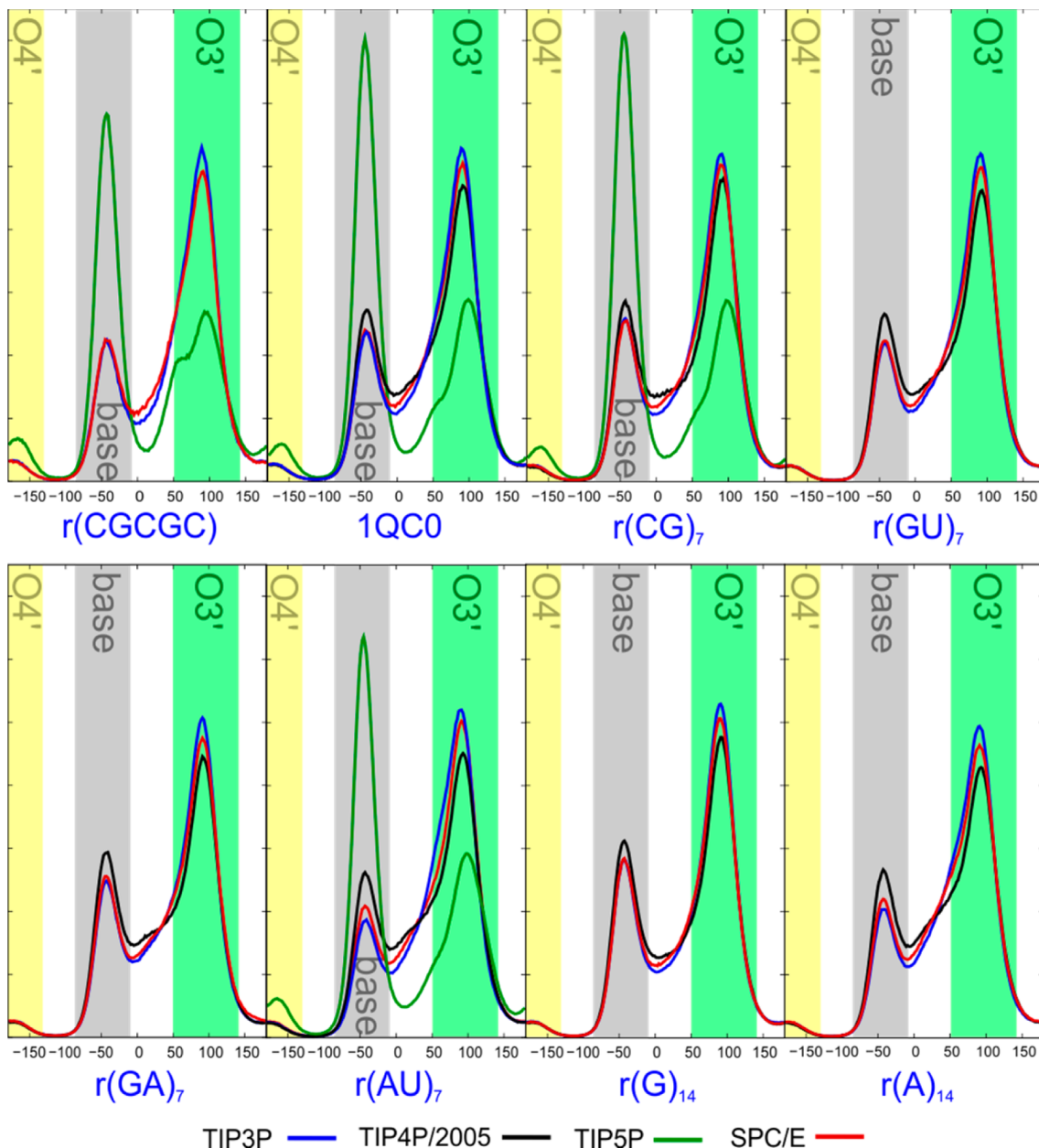


Figure 2. Distribution of the $\text{H}2'\text{--C}2'\text{--O}2'\text{--H}$ torsion angle for all residues of the studied systems. Note that the TIPSP data were obtained only for simulations of the $r(\text{CGCGC})$, $1\text{QC}0$, $r(\text{CG})_7$, and $r(\text{AU})_7$ duplexes (see Methods).

hydrogen bond to the oxygen of a water molecule when oriented to the base domain, it accepts a hydrogen bond from water hydrogen when in the $\text{O}3'$ or $\text{O}4'$ domains. Thus, the difference in affinity of a water molecule to donate/accept a hydrogen bond to/from the $2'\text{-OH}$ between water models might affect the orientation of the $2'\text{-OH}$ group, and this effect might propagate to the entire RNA structure.

To explicitly test the suspected effect of the water model choice on the $2'\text{-OH}$ orientation, and consequently, on the entire RNA structure, we measured the distribution of the $\text{H}2'\text{--C}2'\text{--O}2'\text{--2'}\text{OH}$ torsion angle documenting the $2'\text{-OH}$ orientation. We indeed observed differences in the orientation of the $2'\text{-OH}$ group among the studied water models. Namely, we found that the distribution of the $2'\text{-OH}$ orientation was similar in all models except TIPSP, which significantly differed from the others. Whereas most of the water models dominantly sampled the $\text{O}3'$ domain, the TIPSP model preferentially

populated the base domain (Figure 2). In addition, we found that TIPSP was also the most deviating water model in terms of the helical parameters (see Figure 3 and Supporting Tables S2, S3, S5). Therefore, we suggest that the large deviation of the helical parameters in simulations using the TIPSP water model from the other water models is most likely caused by the significantly different orientation of the $2'\text{-OH}$ group.

According to NMR studies at low temperatures, the $2'\text{-OH}$ group can be oriented toward either the $\text{O}3'$ or base domains, but the $\text{O}3'$ domain is rather dominantly populated.⁷⁴ This fact, together with the large deviation of helical parameters predicted by the TIPSP simulations relative to X-ray values (and also compared with simulations with other water models), suggests that the TIPSP model does not correctly describe the solvation of RNA and thus cannot be recommended for RNA simulations (henceforth, we refrain from discussing the data from the TIPSP simulations).

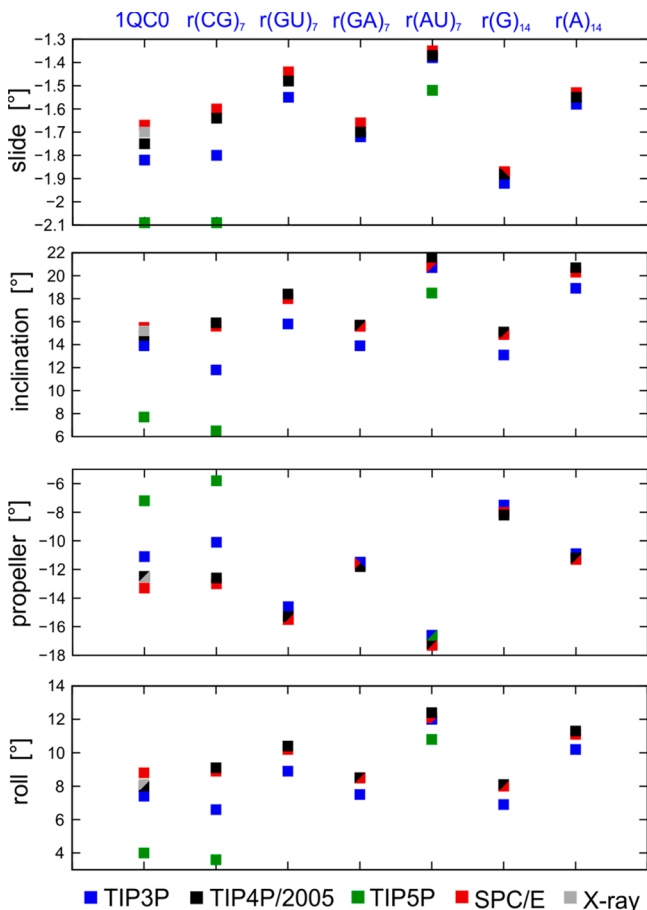


Figure 3. Representative mean structural parameters of the studied RNA duplexes calculated for the inner 10 or 6 base pair segments over complete simulations of repetitive duplexes or the 1QC0 system, respectively. A description of the helical parameters, estimation of errors, and corresponding values of helical parameters decomposed for base pair steps are given in the Supporting Information (Figures S3 and S4 and Table S5, respectively).

Influence of the Water Model on the Structural Parameters of the Studied Systems. To explore the effects of the explicit water models on the behavior of A-RNA structural dynamics in more detail, we performed simulations of RNA duplexes with repetitive sequences ($r(CG)_7$, $r(AU)_7$, $r(GA)_7$, $r(GU)_7$, $r(G)_{14}$, and $r(A)_{14}$), part of the 1QC0 duplex, and a short $r(CGCGC)$ duplex using four different explicit solvent models (TIP3P, TIP4P/2005, TIP5P, and SPC/E, see Methods).

The simulations revealed that the predicted helical parameters were sensitive to the explicit water model used, although the magnitude of the sensitivity was different for different sequences (Figure 3). This is consistent with our earlier more limited set of calculations performed with just TIP3P and SPC/E solvents.³⁶ The most sensitive helical parameters were found to be the inclination and roll, which are mathematically interrelated (base pair roll arises from base pair inclination upon helical twisting), slide, ribose pucker, and propeller twist (Figure 3). Note that we did not observe any effect of the water model on base pair opening. The effects of the used explicit water models followed the same trends for all studied A-RNA duplexes; e.g., the TIP3P model gave the lowest inclination of all water models for all sequences. The TIP5P model significantly deviated from X-ray values for the 1QC0

structure (Figure 3). On the other hand, comparison of the performance of the remaining water models was complicated by the fact that the deviations from X-ray values were of comparable magnitude to the effects of crystal packing reported by Besseova et al.³⁸ and the limited number of sufficiently long experimental duplex structures reported (note that only one X-ray structure was used in this study).

To test whether the observed effect of the water model choice was independent of ionic conditions, including the presence of divalent ions, we performed a set of simulations using different ion/water conditions (for more information about the simulation setup, see the Methods section).^{75,76} We found that the effects of water model choice and ionic conditions on helical structure were mutually independent; i.e., the trends observed in the effect of water model choice were independent of ionic conditions and vice versa (Table S2). Consistent with our recent observations, the effect of ionic conditions was smaller than the effect of water model choice.³⁶ This remained true even for simulations with 150 mM KCl with 20 mM Mg_2Cl , i.e., in the presence of divalent ions. However, it should be mentioned that divalent ions are poorly described by approximative nonpolarizable force fields. Thus, it is generally better to avoid their usage in classical MD simulations when they do not play any significant structural role and monovalent ions can be used instead.^{31,77} In addition, contemporary classical simulation on a microsecond time scale can hardly sample the interconversions of Mg^{2+} ions between outer-shell and inner-shell coordination to the phosphates as the residency time of water molecules in the first coordination shell of a Mg^{2+} ion is $\sim 1.5 \mu s$, according to the NMR studies.⁷⁶ In our simulations, we indeed found that depending on the starting positions of divalent ions, such ions might stick to the sugar-phosphate backbone and form frequent single inner-shell or even double inner-shell contacts, i.e., forming a bridge between two phosphate groups across the major groove, which significantly affect the helical parameters of an A-RNA duplex. On the other hand, these frequent single or double inner-shell contacts are a consequence of initial close contact of Mg^{2+} ions to the phosphates and thus should be considered as an artifact. In simulations with only outer-shell coordinated Mg^{2+} ions, the presence of divalent ions did not have any additional effect on the helical structure compared to the simulations with 150 mM KCl salt excess. Finally, we analyzed the effects of the water model choice on the size of the A-RNA duplex by utilizing small $r(CG)_5$ and $r(CGCGC)$ duplexes. We found that the effects of the water model choice declined with decreasing size of the duplex and almost vanished in the case of the pentamer $r(CGCGC)$ duplex (see Tables S3, S4, and S5 in the Supporting Information). Thus, our results suggest that the effect of the water model choice on helical parameters is only apparent for systems with well-defined specific solvation (namely, minor groove solvation, as shown in ref 36), i.e., for long duplexes. In contrast, in short duplexes, the end effects to some extent perturb the specific sequence dependent solvation of the minor groove, which in turn diminishes the water model effect. In addition, the effect of duplex size was largest in the TIP3P water model, whereas the end effects were smaller in the other solvation models (Table S5).

Specific Solvation of the Minor Groove of RNA Duplexes. Let us analyze the source of the sequence dependent correlation between the water model choice and A-RNA structural parameters (Figure 3). The simulation data suggested that the helical parameters were interrelated with the distance

between the O_{2'} atoms across the base pair step in the minor groove. For instance, the correlation coefficient for the interrelation between the O_{2'...}O_{2'} distance and inclination in the r(CG)₇-tract using the TIP3P model was $r = 0.607 \pm 0.002$; cf. Figures 4 and 5 with Figure 3. The mean O_{2'...}O_{2'}

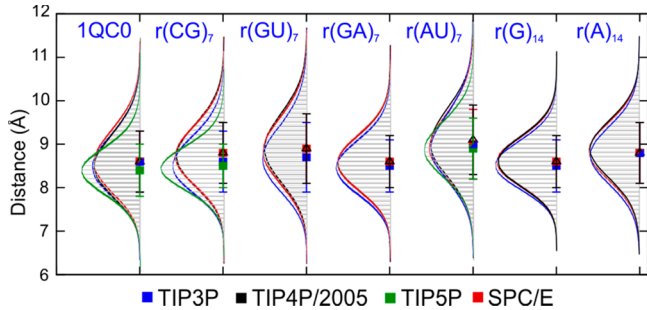


Figure 4. Histogram showing the distance between the 2'-hydroxyl groups (i.e., O_{2'...}O_{2'} distance) of the studied systems in different explicit solvents showing the mean and standard deviation (mean \pm sigma). TIP5P data are shown only for three systems. Note that the mean values for TIP4P/2005 are depicted by a black triangle instead of squares for clarification as the TIP4P/2005 data often overlaps with SPC/E. A description of the O_{2'...}O_{2'} distance is given in the Supporting Information (Figure S5).

distance and mean inclination increased in the order TIP5P < TIP3P < SPC/E \approx TIP4P/2005 (the correlation coefficient between the mean O_{2'...}O_{2'} distance and mean inclination in the r(CG)₇-tract simulations with different water models was $r = 0.9182 \pm 0.0006$; Figures 3 and 4). Similarly, the mean O_{2'...}O_{2'} distance is also positively correlated with the inclination for different duplexes (the correlation coefficient between mean O_{2'...}O_{2'} distance and mean inclination in the TIP3P simulations among different duplexes was $r = 0.9708 \pm 0.0002$). The MD simulations suggested that a sufficiently long RNA duplex establishes a specific solvation pattern in its minor

groove, which includes water bridging between the 2'-OH groups across the minor groove. As a consequence, different parametrizations of the water model (affecting the propensity of a given water model to form firmly bound water bridges) and presumably also different RNA sequences might result in different patterns of water molecules bridging the 2'-OH groups and hence different average values of the O_{2'...}O_{2'} distance. Assuming that base pair steps tend to preserve the stacking overlap between neighboring base pairs, the increased distance between the 2'-OH groups most likely results in increased slide, inclination, and roll (Figure 6B).

Let us first investigate the (sequence dependent) effect of the water model choice. We analyzed specific solvation of the minor groove in the set of r(CG)₇ and r(AU)₇ tract simulations, which showed the largest and lowest sensitivity of the A-RNA structure to the water model, respectively. The existence of a complex hydration network spanning the minor groove of an RNA A-form helix has previously been suggested from a high resolution X-ray study of an RNA duplex.¹⁴ Both electron density maps in X-ray crystallography and water density maps obtained by MD simulations indicate that a typical feature of A-RNA minor groove hydration is the formation of structural water molecules spanning the 2'-hydroxyl groups of ribose moieties from the opposite strands of a given base pair across the minor groove (see Figure S6 for X-ray and MD density maps).¹⁵ However, detailed analysis of our simulation data showed that the situation is more complex than previously suggested.¹⁴ Water density maps obtained from both X-ray crystallography and MD clearly show regions of locally increased water density and thus presumably identify regions carrying tightly bound water molecule(s).^{6,7,11,18} However, it seems that none of these regions can be attributed to a single water molecule tightly bound by a well-defined hydrogen bonding pattern. Instead, we observed dynamical hydration of the minor groove, which can be described as an ensemble of specific hydration patterns that together give rise to regions of

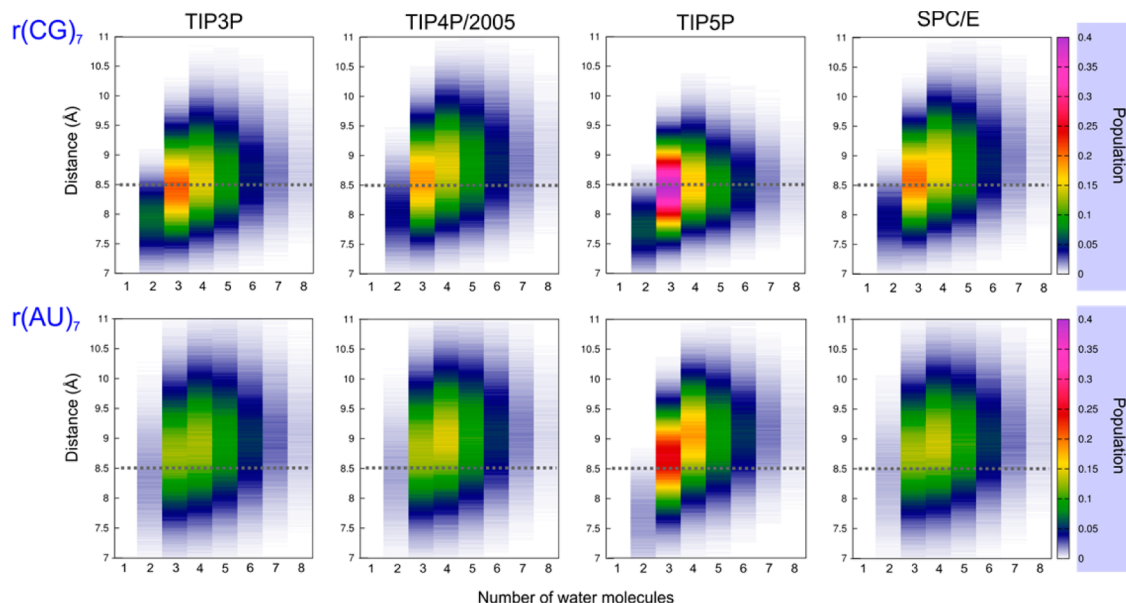


Figure 5. Normalized density maps showing the population of the distance between the 2'-hydroxyl groups vs number of water molecules connecting the 2'-hydroxyl groups via an uninterrupted H-bond network calculated over the entire trajectory of r(CG)₇ and r(AU)₇ RNA duplexes for each explicit water model. As an example, the dashed gray line shows a distance of 8.5 Å that is close to the second peak, i.e., density maximum of the state connected by three water molecules.

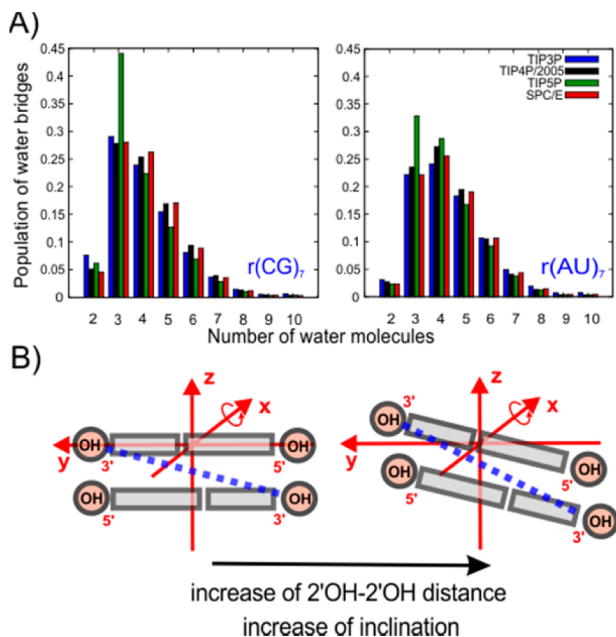


Figure 6. (A) Population of states for a given number of water molecules connecting the 2'-hydroxyl groups of $r(CG)_7$ and $r(AU)_7$ RNA duplexes, using H-bonds calculated over 200 ns for each water model. (B) Schematic of the relationship between inclination and distance between the 2'-OH groups across the minor groove.

increased electron and/or water densities (see also the rather wide distribution of the number of water molecules bridging the two 2'-OH groups across the minor groove, Figure 6A).

The above discussion suggests that the widely used analysis of minor groove hydration patterns based on density maps may be insufficient or even misleading. Instead, we focused on the distribution of the number of water molecules connecting the 2'-hydroxyl groups across the minor groove. Our simulations showed that the 2'-hydroxyl groups (each from a different strand and base pair within a base pair step, see Figure 6B) are connected via an uninterrupted chain of hydrogen bonded waters, which most often involves three water molecules (Figures 5 and 6A). Figure 5 shows population histograms of the O_{2'}...O_{2'} distances in states where these two groups are connected by a continuous hydration pattern involving n bridging water molecules. Note that regardless of the water model choice and sequence, the mean O_{2'}...O_{2'} distance was $\sim 8.0 \text{ \AA}$, $\sim 8.5 \text{ \AA}$, and $\sim 9.0 \text{ \AA}$ in states with two, three, and more than three bridging waters, respectively (see Supporting Information Figure S9 for the orientations of the 2'-OH groups for $r(CG)_7$ and $r(AU)_7$ tracts in states with two or three bridging waters). Thus, an increased population of states with two (or to some extent also three) bridging water molecules should result in decreased O_{2'}...O_{2'} distances. We found that the simulation of $r(CG)_7$ with the TIP3P water model showed a higher population of two and/or three bridging water molecules in comparison with simulations with the TIP4P/2005 and SPC/E water models (Figures 6A and 7). Thus, such an increased population of states bridged by two or three waters might explain the observed decrease in O_{2'}...O_{2'} distance and corresponding decrease in inclination, slide, and roll parameters for the TIP3P model. Note that the decreased population of states with three and more bridging water molecules for TIP3P might be caused by an inability of this water model to correctly describe complex structures of waters,

as suggested by the lack of second and higher peaks in the goo radial distribution function in bulk water. On the other hand, the populations of two or three bridging water molecules were significantly smaller in the $r(AU)_7$ simulations than in the case of $r(CG)_7$. Thus, although the relative trends between water models were similar in both sequences (see the population of the state with two bridging water molecules, which has the most significant effect on O_{2'}...O_{2'} distance, Figure 6A), the influence of the water model on the O_{2'}...O_{2'} distance was diminished in $r(AU)_7$ due to the relatively low population of the two waters in the bridge. Hence, the results suggest that the number of water molecules bridging the 2'-hydroxyl groups (especially the population of the state with two waters in the bridge) affects the distance between the hydroxyl groups and, as a consequence, also the inclination, roll, and slide. Note that whereas the water model choice fine-tunes the extent of water bridging between the 2'-OH groups, the sequence seems to play a dominant role. Thus, the propensity of each sequence to establish specific hydration patterns with two waters forming a bridge between 2'-OH groups across the minor groove could explain the different sensitivity of these sequences to the water model choice.

For the sake of completeness, we would like to comment on the effect of minor groove solvation on the propeller angle, which is the remaining helical parameter affected by the water model choice. By overlapping the backbone of the snapshots from the simulations with different propeller angles, we found that a shift of the propeller angle led to displacement of the atoms in the major groove, while the minor groove atoms remained unaffected. In our previous study,³⁶ we showed that the sensitivity of helical parameters (including propeller angle) to water model choice is modulated by the presence or absence of a purine minor groove N2 amino group rather than any modifications in the major groove. This indicates that an increase in propeller angle is rather a secondary consequence of increased inclination and roll, as presumably the base pair step tends to maximize stacking upon increased inclination and roll by modifying the propeller angle. Increased roll reduces intrastrand stacking, which can be improved by propeller twisting, while at the same time reducing the severity of interstrand minor groove amino group steric clashes caused by propeller twisting.⁷⁸

Effect of Sequence on the Helical Structure of A-RNA Duplexes. Stacking or Hydration Effect? The exact determination of the origin of the dependence of the A-RNA structure on sequence is not straightforward. In a recent study,³⁶ we showed that the helical structure, as well as its sensitivity to water model choice, did not change upon substitution of AU to inosine/cytosine (IC) or GC to diaminopurine/uracile (DU) base pairs. In other words, the helical parameters and their sensitivity to water model choice are only affected by the steric shape of base pairs and/or presence or absence of an N2-exocyclic amino group(s) in the minor groove. We suggested that these findings could most likely be explained by steric effects (i.e., steric effect of intramolecular stacking between base pairs, which is the traditional rationalization resembling the Dickerson–Calladine rules of B-DNA sequence variability).^{79,80} However, we also acknowledged the potential role of minor groove hydrogen bonding patterns in affecting the specific minor groove solvation. Unfortunately, studies of different real A-RNA systems cannot provide an unambiguous answer, as real molecules do not allow separation of the steric and hydration

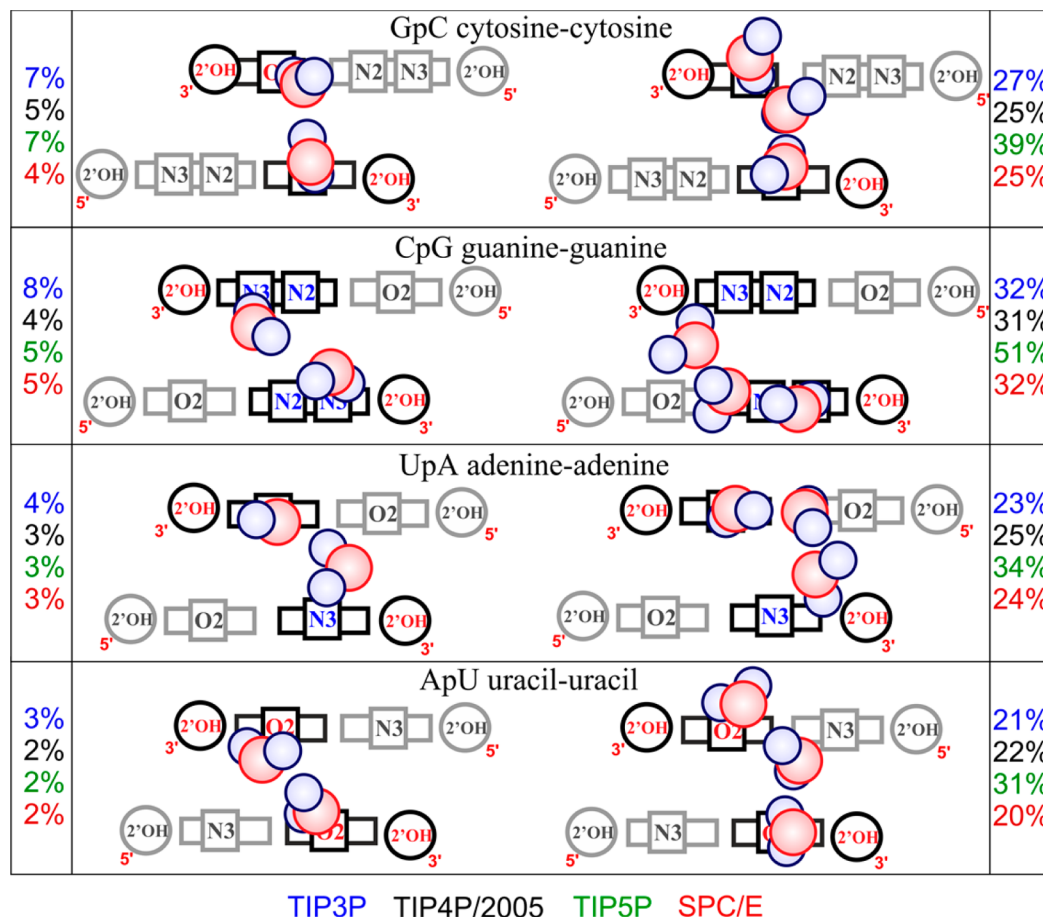


Figure 7. Scheme showing the position of water molecules in the minor groove of hydration patterns with two or three waters forming a bridge between 2'-OH hydroxyls in different base pair steps. The figures are based on representative MD snapshots (see Supporting Information Figure S8 for the original snapshots). The numbers indicate the percentage population for each hydration pattern obtained during the MD simulations (see also Figure 6).

effects associated with the purine minor groove amino groups. Thus, we tried to resolve the issue by simulating an artificial system where steric stacking effects can be separated from minor groove hydration.

As demonstrated above, different populations of distinct hydration patterns could explain the sensitivity of the A-RNA structure to the water model. Thus, it seems plausible to suggest that the sequence dependence of the A-RNA structure, which is a real effect, may also be affected by hydration effects. Namely, different hydrogen bonding patterns in the minor groove (three or two hydrogen bond donors/acceptors per GC or AU base pair, respectively) might result in different specific solvation of the minor groove with different populations of states with two or three waters bridging the 2'-OH groups across the minor groove (see Figure 6), which in turn affects the inclination, roll, and slide.

To test this hypothesis (sequence dependence due to intramolecular stacking or minor groove solvation), we performed a simulation of a hybrid r(A/D)₁₄-tract. This hybrid system is the same as a r(A)₁₄-tract but with explicit inclusion of an N2-exocyclic amino group in the RNA–RNA van der Waals term. Therefore, water molecules sense the system exactly as a pure r(A)₁₄-tract, whereas in terms of van der Waals stacking, it behaves as a r(D)₁₄-tract (with DU instead of AU base pairs, see Methods and Supporting Information). This simulation thus mimicked the A-tract hydration effects and electrostatic

stacking but with an additional stacking steric effect of the minor groove amino group (note that the water molecules do not sense this added bulky group, as it is included only in calculations of the van der Waals part of base stacking). Although this simulation is completely unphysical, it can be used to separate the contributions of intramolecular stacking and minor groove solvation to the sequence dependence of the helical structure of A-RNA. If the steric part of intramolecular stacking is primarily responsible for the sequence dependence of the helical structure, such hybrid simulations should behave like an r(D)₁₄-tract. In contrast, if minor groove solvation is responsible for the sequence dependence, the hybrid simulations should resemble the structural features of the r(A)₁₄-tract. Indeed, we found that the hybrid r(A/D)₁₄-tract exhibited inclination and roll parameters very close to the r(A)₁₄-tract simulation, which suggests that minor groove solvation dominantly contributes to the observed sequence dependence of the inclination, roll, and slide (Figure 8).

Note that during these simulations, the conformations of AU, DU, and (A/D)U base pairs were restrained to be close to the conformation of a DU base pair (this was required in the case of the hybrid r(A/D)₁₄-tract due to technical reasons and was also used for the r(A)₁₄-tract and r(D)₁₄-tract simulations to test the effect of these restraints, see Methods and Supporting Information). We found that the unrestrained simulation of the r(A)₁₄-tract revealed a slightly increased inclination and roll

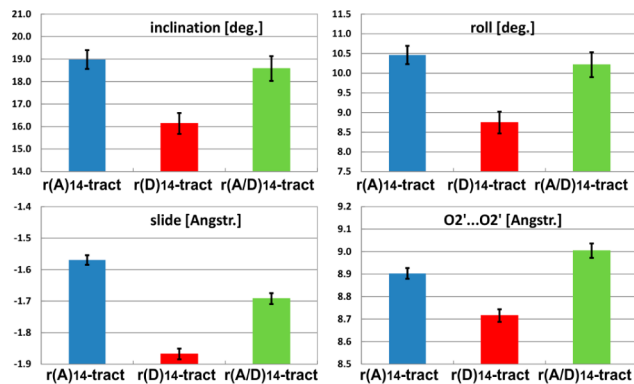


Figure 8. Mean inclination, roll, and slide helical parameters and mean O2'...O2' distance across the minor groove of a base pair step (see Figure 6B) in r(A)₁₄-tract, r(D)₁₄-tract, and hybrid r(A/D)₁₄-tract simulations averaged over time for the 10 base pair internal part of the duplexes. The error bars are calculated as confidence intervals for mean value estimation (using decorrelation of the data set into 50 2-ns-long frames).

compared to the restrained simulations, whereas the effect of restraints on the r(D)₁₄-tract was rather negligible (see Figures 3 and S2). This might be explained by a modest change in the AU base pair conformation upon applying the restraints. Despite the fact that the AU base pair conformation was assumed to be isosteric with a DU base pair (similar to the isostericity between AU and GC), small differences between the AU and DU geometries were evident in our unrestrained simulations (see histograms of the A/D(C2)...U(C2) distance in Figure S7). Thus, we suggest that a small part of the sequence dependence can be attributed to a change of the base pair geometry. Finally, note that the slide value for the hybrid r(A/D)₁₄-tract lay between the mean slide values of the r(D)₁₄-tract and r(A)₁₄-tract, which suggests that in the case of slide, some effect of base stacking was sensed.

Unfortunately, an analogous simulation with the r(D/A)₁₄ hybrid tract (r(D)₁₄-tract-like solvation and r(A)₁₄-tract-like RNA–RNA interactions) was not possible as it would require exposure of the amino group point charges without their van der Waals spheres, which would break down the simulations.

Taken together, our results suggest that both the spurious dependence of the helical parameters on the choice of water model as well as the observed sequence dependence of the helical A-RNA structure primarily originate from the relationship between specific sequence dependent minor groove solvation, number of bridging waters between 2'-OH groups across the minor groove, O2'...O2' distance, and the helical parameters inclination, roll, and slide. Note that this finding cannot be straightforwardly applied for the prediction of helical parameters of an A-RNA duplex as a function of sequence as the influence of nearest neighbor effects on the specific solvation of the minor groove is still unknown and because of the lack of experimental structural data available, as discussed above. Instead, we argue that besides the traditional interpretation that the sequence dependence of helical structure is due to intrinsic stacking, specific solvation also needs to be taken into account and, furthermore, in the case of an A-RNA duplex, might dominate over the intrinsic stacking. In addition, our findings help to explain why water molecules solvating the RNA stem should be considered an integral part of an A-RNA duplex.

CONCLUSIONS

We carried out a MD study of A-RNA duplexes of different sequences using four explicit water models to examine the influence of the explicit water model and sequence on the structural parameters of RNA helices.

We found that both the sequence and choice of explicit water model affected the helical parameters of A-form duplexes (namely, inclination, roll, and slide) via modulation of the minor groove specific hydration; the hydration pattern between the 2'-OH groups across the minor groove influences the distance between the 2'-OH groups and, consequently, the above-mentioned helical parameters.

The overall hydration pattern should be considered as a complex ensemble of a number of competing hydration patterns with a variable number of water molecules in the water-bridge network. This suggests that analysis of hydration patterns based on electron (water) densities is not fully sufficient to capture the RNA structural hydration, despite being widely used.

The sequence dependence of nucleic acid double helices is usually attributed to base stacking. However, our work suggests that the sequence dependent variations of the helical parameters of A-RNA should rather be explained by considering the structural effects of explicit waters in the minor groove and varying populations of different types of water bridges. These waters should be considered as an integral part of the RNA structure, albeit they do not represent any tightly bound waters. We suggest that implicit solvent models cannot adequately describe such specific solvation effects and the sequence dependence of nucleic acids helical parameters. Our study demonstrates that the local conformational variability of nucleic acid double helices is a complex issue which is not determined solely by base stacking. In fact, in the case of A-RNA, the dynamical minor groove water network may be more important than variations of stacking, due to the presence of the 2'-OH groups in the minor groove.

We found that the TIP3P, TIP4P/2005, and SPC/E models provide rather consistent results. However, the TIPSP model in combination with the Cornell et al. type of RNA force field leads to incorrect orientation of the 2'-OH groups and subsequent unsatisfactory conformational description of the simulated RNAs.^{33,61,62}

ASSOCIATED CONTENT

S Supporting Information

The Supporting Information provides simulation details, details of the hybrid r(A/D)₁₄-tract simulations, and helical parameters of all duplexes used in this study, including the small r(CGCGC) tract. This material is available free of charge via the Internet at <http://pubs.acs.org>.

AUTHOR INFORMATION

Corresponding Author

*Phone +420 585634769. E-mail: pavel.banas@upol.cz.

Notes

The authors declare no competing financial interest.

ACKNOWLEDGMENTS

This work was funded by the grants P208/12/1878 (J.S., M.O., P.K.) and P301/11/P558 (P.B.) from the Czech Science Foundation. This work was further supported by the project “CEITEC – Central European Institute of Technology”

CZ.1.05/1.1.00/02.0068 from the European Regional Development Fund (J.S.), the Operational Program Research and Development for Innovations – European Regional Development Fund (project CZ.1.05/2.1.00/03.0058), the Operational Program Education for Competitiveness – European Social Fund (CZ.1.07/2.3.00/20.0017) of the Ministry of Education, Youth and Sports of the Czech Republic (P.K., M.O., P.B.), and by student project PrF_2013_028 of Palacky University (M.O., P.B.).

■ REFERENCES

- (1) Ball, P. *Chem. Rev.* **2008**, *108*, 74–108.
- (2) Denisov, V. P.; Carlstrom, G.; Venu, K.; Halle, B. *J. Mol. Biol.* **1997**, *268*, 118–136.
- (3) Phan, A. T.; Leroy, J. L.; Gueron, M. *J. Mol. Biol.* **1999**, *286*, 505–519.
- (4) Pal, S.; Maiti, P. K.; Bagchi, B.; Hynes, J. T. *J. Phys. Chem. B* **2006**, *110*, 26396–26402.
- (5) Feig, M.; Pettitt, B. M. *Biophys. J.* **1999**, *77*, 1769–1781.
- (6) Auffinger, P.; Westhof, E. *J. Mol. Biol.* **2000**, *300*, 1113–1131.
- (7) Auffinger, P.; Westhof, E. *J. Mol. Biol.* **2001**, *305*, 1057–1072.
- (8) Reblova, K.; Spackova, N.; Stefl, R.; Csaszar, K.; Koca, J.; Leontis, N. B.; Sponer, J. *Biophys. J.* **2003**, *84*, 3564–3582.
- (9) Westhof, E. *Annu. Rev. Biophys. Biophys. Chem.* **1988**, *17*, 125–44.
- (10) Woese, C. R.; Winker, S.; Gutell, R. R. *Proc. Natl. Acad. Sci. U. S. A.* **1990**, *87*, 8467–8471.
- (11) Auffinger, P.; Westhof, E. *J. Biomol. Struct. Dyn.* **1998**, *16*, 693–707.
- (12) Sundaralingam, M.; Pan, B. C. *Biophys. Chem.* **2002**, *95*, 273–282.
- (13) Kirillova, S.; Carugo, O. *BMC Struct. Biol.* **2011**, *11*, 41.
- (14) Adamiak, D. A.; Milecki, J.; Adamiak, R. W.; Rypniewski, W. *New J. Chem.* **2010**, *34*, 903–909.
- (15) Egli, M.; Portmann, S.; Usman, N. *Biochemistry* **1996**, *35*, 8489–8494.
- (16) Leitner, D. M.; Gruebele, M.; Havenith, M. *HFSP J.* **2008**, *2*, 314–323.
- (17) Auffinger, P.; Hashem, Y. *Curr. Opin. Struct. Biol.* **2007**, *17*, 325–333.
- (18) Auffinger, P.; Westhof, E. *Biopolymers* **2001**, *56*, 266–274.
- (19) Krasovska, M. V.; Sefcikova, J.; Reblova, K.; Schneider, B.; Walter, N. G.; Sponer, J. *Biophys. J.* **2006**, *91*, 626–638.
- (20) Yonetani, Y.; Kono, H. *Biophys. Chem.* **2012**, *160*, 54–61.
- (21) Sorin, E. J.; Rhee, Y. M.; Pande, V. S. *Biophys. J.* **2005**, *88*, 2516–2524.
- (22) Paschek, D.; Day, R.; Garcia, A. E. *Phys. Chem. Chem. Phys.* **2011**, *13*, 19840–19847.
- (23) Roy, S.; Bagchi, B. *J. Phys. Chem. B* **2012**, *116*, 2958–2968.
- (24) Bhattacharjee, N.; Biswas, P. *Biophys. Chem.* **2011**, *158*, 73–80.
- (25) Reblova, K.; Spackova, N.; Koca, J.; Leontis, N. B.; Sponer, J. *Biophys. J.* **2004**, *87*, 3397–3412.
- (26) Kriz, Z.; Otyepka, M.; Bartova, I.; Koca, J. *Proteins* **2004**, *55*, 258–274.
- (27) Huggins, D. J. *J. Comput. Chem.* **2012**, *33*, 1383–1392.
- (28) Huggins, D. J. *Phys. Chem. Chem. Phys.* **2012**, *14*, 15106–15117.
- (29) Fadda, E.; Woods, R. J. *J. Chem. Theory Comput.* **2011**, *7*, 3391–3398.
- (30) Egli, M.; Tereshko, V.; Teplova, M.; Minasov, G.; Joachimiak, A.; Sanishvili, R.; Weeks, C. M.; Miller, R.; Maier, M. A.; An, H. Y.; Cook, P. D.; Manoharan, M. *Biopolymers* **1998**, *48*, 234–252.
- (31) Ditzler, M. A.; Otyepka, M.; Sponer, J.; Walter, N. G. *Acc. Chem. Res.* **2010**, *43*, 40–47.
- (32) Sponer, J.; Mladek, A.; Sponer, J. E.; Svozil, D.; Zgarbova, M.; Banas, P.; Jurecka, P.; Otyepka, M. *Phys. Chem. Chem. Phys.* **2012**, *14*, 15257–15277.
- (33) Zgarbova, M.; Otyepka, M.; Sponer, J.; Mladek, A.; Banas, P.; Cheatham, T. E.; Jurecka, P. *J. Chem. Theory Comput.* **2011**, *7*, 2886–2902.
- (34) Krepl, M.; Zgarbova, M.; Stadlbauer, P.; Otyepka, M.; Banas, P.; Koca, J.; Cheatham, T. E.; Jurecka, P.; Sponer, J. *J. Chem. Theory Comput.* **2012**, *8*, 2506–2520.
- (35) Zgarbova, M.; Luque, F. J.; Sponer, J.; Cheatham, T. E.; Otyepka, M.; Jurecka, P. *J. Chem. Theory Comput.* **2013**, *9*, 2339–2354.
- (36) Besseova, I.; Banas, P.; Kuhrava, P.; Kosinova, P.; Otyepka, M.; Sponer, J. *J. Phys. Chem. B* **2012**, *116*, 9899–9916.
- (37) Sklenovsky, P.; Florova, P.; Banas, P.; Reblova, K.; Lankas, F.; Otyepka, M.; Sponer, J. *J. Chem. Theory Comput.* **2011**, *7*, 2963–2980.
- (38) Besseova, I.; Otyepka, M.; Reblova, K.; Sponer, J. *Phys. Chem. Chem. Phys.* **2009**, *11*, 10701–10711.
- (39) Guillot, B. *J. Mol. Liq.* **2002**, *101*, 219–260.
- (40) Finney, J. L. *J. Mol. Liq.* **2001**, *90*, 303–312.
- (41) Banas, P.; Walter, N. G.; Sponer, J.; Otyepka, M. *J. Phys. Chem. B* **2010**, *114*, 8701–8712.
- (42) Rick, S. W. *J. Chem. Phys.* **2001**, *114*, 2276–2283.
- (43) van der Spoel, D.; van Maaren, P. J.; Berendsen, H. J. C. *J. Chem. Phys.* **1998**, *108*, 10220–10230.
- (44) Mahoney, M. W.; Jorgensen, W. L. *J. Chem. Phys.* **2000**, *112*, 8910–8922.
- (45) Glattli, A.; Daura, X.; van Gunsteren, W. F. *J. Chem. Phys.* **2002**, *116*, 9811–9828.
- (46) Burnham, C. J.; Xantheas, S. S. *J. Chem. Phys.* **2002**, *116*, 1479–1492.
- (47) Yu, H. B.; van Gunsteren, W. F. *J. Chem. Phys.* **2004**, *121*, 9549–9564.
- (48) Olano, L. R.; Rick, S. W. *J. Comput. Chem.* **2005**, *26*, 699–707.
- (49) Saint-Martin, H.; Hess, B.; Berendsen, H. J. C. *J. Chem. Phys.* **2004**, *120*, 11133–11143.
- (50) Jorgensen, W. L.; Chandrasekhar, J.; Madura, J. D.; Impey, R. W.; Klein, M. L. *J. Chem. Phys.* **1983**, *79*, 926–935.
- (51) Mahoney, M. W.; Jorgensen, W. L. *J. Chem. Phys.* **2001**, *114*, 363–366.
- (52) Berendsen, H. J. C.; Grigera, J. R.; Straatsma, T. P. *J. Phys. Chem.* **1987**, *91*, 6269–6271.
- (53) Florova, P.; Sklenovsky, P.; Banas, P.; Otyepka, M. *J. Chem. Theory Comput.* **2010**, *6*, 3569–3579.
- (54) Nutt, D. R.; Smith, J. C. *J. Chem. Theory Comput.* **2007**, *3*, 1550–1560.
- (55) Shirts, M. R.; Pande, V. S. *J. Chem. Phys.* **2005**, *122*, No. 144107.
- (56) Glass, D. C.; Krishnan, M.; Nutt, D. R.; Smith, J. C. *J. Chem. Theory Comput.* **2010**, *6*, 1390–1400.
- (57) Wong, V.; Case, D. A. *J. Phys. Chem. B* **2008**, *112*, 6013–6024.
- (58) Nerenberg, P. S.; Head-Gordon, T. *J. Chem. Theory Comput.* **2011**, *7*, 1220–1230.
- (59) Pearlman, D. A.; Case, D. A.; Caldwell, J. W.; Ross, W. S.; Cheatham, T. E.; Debolt, S.; Ferguson, D.; Seibel, G.; Kollman, P. *Comput. Phys. Commun.* **1995**, *91*, 1–41.
- (60) Banas, P.; Hollas, D.; Zgarbova, M.; Jurecka, P.; Orozco, M.; Cheatham, T. E.; Sponer, J.; Otyepka, M. *J. Chem. Theory Comput.* **2010**, *6*, 3836–3849.
- (61) Cornell, W. D.; Cieplak, P.; Bayly, C. I.; Gould, I. R.; Merz, K. M.; Ferguson, D. M.; Spellmeyer, D. C.; Fox, T.; Caldwell, J. W.; Kollman, P. *A. J. Am. Chem. Soc.* **1996**, *118*, 2309–2309.
- (62) Perez, A.; Marchan, I.; Svozil, D.; Sponer, J.; Cheatham, T. E.; Laughton, C. A.; Orozco, M. *Biophys. J.* **2007**, *92*, 3817–3829.
- (63) Abascal, J. L. F.; Vega, C. *J. Chem. Phys.* **2005**, *123*, No. 234505.
- (64) Joung, I. S.; Cheatham, T. E. *J. Phys. Chem. B* **2008**, *112*, 9020–9041.
- (65) Allner, O.; Nilsson, L.; Villa, A. *J. Chem. Theory Comput.* **2012**, *8*, 1493–1502.
- (66) Banas, P.; Sklenovsky, P.; Wedekind, J. E.; Sponer, J.; Otyepka, M. *J. Phys. Chem. B* **2012**, *116*, 12721–12734.
- (67) Mlynšky, V.; Banas, P.; Hollas, D.; Reblova, K.; Walter, N. G.; Sponer, J.; Otyepka, M. *J. Phys. Chem. B* **2010**, *114*, 6642–6652.
- (68) Klosterman, P. S.; Shah, S. A.; Steitz, T. A. *Biochemistry* **1999**, *38*, 14784–14792.
- (69) Lu, X. J.; Olson, W. K. *Nucleic Acids Res.* **2003**, *31*, 5108–5121.

- (70) Banas, P.; Mladek, A.; Otyepka, M.; Zgarbova, M.; Jurecka, P.; Svozil, D.; Lankas, F.; Sponer, J. *J. Chem. Theory Comput.* **2012**, *8*, 2448–2460.
- (71) Spasic, A.; Serafini, J.; Mathews, D. H. *J. Chem. Theory Comput.* **2012**, *8*, 2497–2505.
- (72) Auffinger, P.; Westhof, E. *J. Mol. Biol.* **1997**, *274*, 54–63.
- (73) Leontis, N. B.; Stombaugh, J.; Westhof, E. *Nucleic Acids Res.* **2002**, *30*, 3497–3531.
- (74) Nozinovic, S.; Furtig, B.; Jonker, H. R. A.; Richter, C.; Schwalbe, H. *Nucleic Acids Res.* **2010**, *38*, 683–694.
- (75) Li, W. F.; Nordenskiold, L.; Mu, Y. G. *J. Phys. Chem. B* **2011**, *115*, 14713–14720.
- (76) Bleuzen, A.; Pittet, P. A.; Helm, L.; Merbach, A. E. *Magn. Reson. Chem.* **1997**, *35*, 765–773.
- (77) Banas, P.; Jurecka, P.; Walter, N. G.; Sponer, J.; Otyepka, M. *Methods* **2009**, *49*, 202–216.
- (78) Sponer, J.; Kypr, J. *J. Mol. Biol.* **1991**, *221*, 761–764.
- (79) Calladine, C. R. *J. Mol. Biol.* **1982**, *161*, 343–352.
- (80) Dickerson, R. E. *Biophys. J.* **1983**, *41*, A210–A210.